Inorganic Chemistry

ARTICLE

pubs.acs.org/IC

# Immobilization, Trapping, and Anion Exchange of Perrhenate Ion Using Copper-Based Tripodal Complexes

Rui Cao, Brian D. McCarthy, and Stephen J. Lippard*

Department of Chemistry, Massachusetts Institute of Technology, Cambridge, Massachusetts 02139, United States.

Supporting Information

**ABSTRACT:**

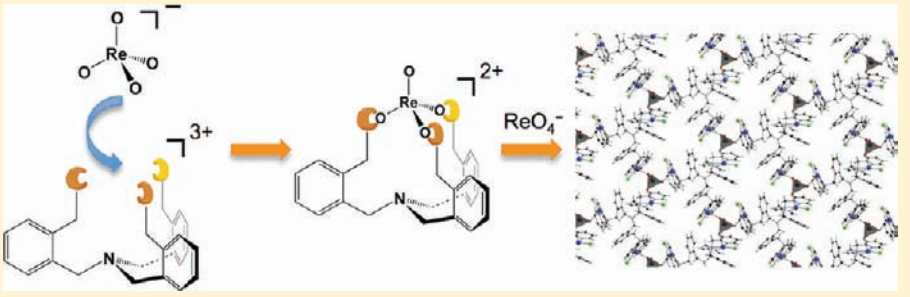


We describe a multidentate tripodal ligand in which three pendant arms carrying di(2-picolyl)amine units are linked to the ortho positions of a tris(*o*-xylyl) scaffold, providing $N(CH_2\text{-}o\text{-}C_6H_4CH_2N(CH_2py)_2)_3$ (**L**). Reaction of **L** with $CuCl_2$ in the presence of hexafluorophosphate anion afforded blue cubes of $[(CuCl)_3\mathbf{L}](PF_6)_3\cdot 5H_2O$ (**1**). Crystallographic studies of **1** revealed that the three symmetry-related arms each coordinate a $\{Cu^{II}Cl\}$ unit, and two molecules of **1** are connected to one another through a $Cu(\mu\text{-}Cl)_2Cu$ bridge, extending the molecular structure to form a two-dimensional (2-D) layer. These 2-D layers pack in an ABCABC... fashion with $PF_6^-$ anions located in between. Reaction of **1** with a stoichiometric amount of perrhenate ion afforded blue plates of $[(CuCl)_3\mathbf{L}](PF_6)(ReO_4)_2\cdot 3H_2O$ (**2**). Compound **2** has the same lattice structure as **1**, but the tricopper unit backbone now traps one $ReO_4^-$ anion through Coulombic interactions. In addition, three molecules of **2** are bridged by a perrhenate ion, forming a $Cu_3(\mu^3\text{-}ReO_4)$ cluster, to give a different 2-D structure displaying a rare tridentate bridging $ReO_4^-$ mode. Thus, in addition to classic perrhenate trapping through weak Coulombic interactions, **2** represents an exceptional example in which the $ReO_4^-$ anion is immobilized in an extended framework through tight covalent interactions. The interlamellar $PF_6^-$ anions in **1** can be exchanged with other anions including perrhenate, perchlorate, or periodate. The structural similarity between perrhenate and pertechnetate makes these materials of potential interest for pertechnetate trapping.

## INTRODUCTION

Systems that trap and immobilize anions have attracted much recent attention.[1−8] Because anions regulate a variety of physiological processes, they are potential toxins. As examples, perchlorate ion can adversely affect human health by interfering with iodide uptake into the thyroid,[9−11] and chromate ($CrO_4^{2-}$) is toxic, mutagenic, and a human carcinogen.[12,13] As a result, many oxohydroxo anionic forms of metals and p-block elements are listed as U.S. EPA priority pollutants.[14] Among anionic pollutants, pertechnetate, the tetrahedral oxoanion of technetium, is especially noteworthy. Apart from its ability to interfere with physiological processes, technetium is a nuclear fission waste product with significant radioactivity. Because of its long half-life and good environmental mobility, pertechnetate is one of the most dangerous radiation-derived contaminants and a major concern for long-term disposal of radioactive waste.

In part because of such issues, chemists are interested to develop methods and materials for trapping anions. Resins with cationic quaternary ammonium polymer chains and exchangeable counteranions are the standard in commercial anion exchangers, although they have limited thermal and chemical stability.[15] Molecular trapping complexes, in particular ion pair receptors with recognition sites for both cations and anions, are able to bind an ion pair through cooperative interactions between co-bound ions.[3,16,17] Layered double hydroxides having the general formula $[M^{2+}_{1-x}M^{3+}_{x}(OH)_2]A^{n-}_{x/n}\cdot mH_2O$, where trivalent metal ions substitute for some of the divalent ones, have a net positive charge on the layered framework. These substances comprise an isostructural class of pure inorganic materials capable of exchanging interlamellar counteranions with other anions of interest.[18−20] Metal−organic frameworks (MOFs) with extended cationic networks and guest anions are also potential candidates for anion exchange and trapping.[6,21−24]

In the foregoing examples, the anions are typically bound through weak electrostatic and/or hydrogen-bonding interactions.

**Received:** May 31, 2011
**Published:** August 26, 2011

**Chart 1**

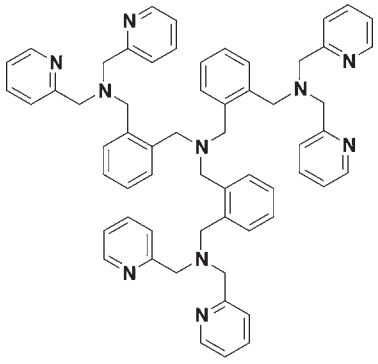

tris-dpa ligand **L**

The binding constants of anions in these systems are small, and this problem is especially troubling for the binding of pertechnetate, which is relatively large and of low charge density and has a small enthalpy of complexation.[2] As a consequence, it has proved difficult to prepare receptors for $TcO_4^-$, and there is a need for new materials that can trap it with high affinity.[2] Recently, we reported a multidentate tripodal ligand, $N(CH_2\text{-}o\text{-}C_6H_4CH_2N(CH_2py)_2)_3$ (**L**), which carries three di(2-picolyl)amine (dpa) units linked to the ortho positions of a tris(*o*-xylyl) scaffold (Chart 1). The reaction of **L** with transition-metal ions produced trinuclear complexes that effectively coordinate tetrahedral oxoanions, such as phosphate and arsenate, with each of the three metal ions coordinated to an O atom of the central $MO_4^{n-}$ anion.[25] As a result, the tridentate bridging tetraoxoanion is immobilized by the trinuclear metal complex via strong covalent bonds.

We therefore decided to explore the potential of the tripodal ligand **L** to bind pertechnetate ion, and the present article describes our findings. As a surrogate for the radioactive $TcO_4^-$ ion, we employed the chemically and structurally similar perrhenate anion, specifically with a Cu(II) complex **1**. The result is an extended, cationic two-dimensional (2-D) structure capable of completely exchanging interlamellar $PF_6^-$ anions with other anions, including perrhenate, perchlorate, and periodate.

## EXPERIMENTAL SECTION

**Synthesis of $N(CH_2\text{-}o\text{-}C_6H_4CH_2N(CH_2py)_2)_3$ (L).** Ligand **L** was synthesized following our published method,[25] and its identity and purity were confirmed by $^1H$ and $^{13}C$ NMR spectroscopy and high-resolution electrospray ionization mass spectrometry (ESI-MS). Crystals of **L** suitable for single-crystal X-ray diffraction were obtained from a dichloromethane (DCM)/hexane (1:5) solution of **L**. Slow evaporation of this solution at −10 °C afforded large colorless prisms of **L** in 3 weeks. Detailed characterization of **L** is available in the Supporting Information, SI.

**Synthesis of $[(CuCl)_3L](PF_6)_3\cdot 5H_2O$ (1).** To a stirred solution of **L** (30.0 mg, 0.032 mmol) in 10 mL of DCM at room temperature was added 14.5 mg of $CuCl_2$ (0.106 mmol, 3.3 equiv) dissolved in 5 mL of MeOH. The resulting clear green-blue solution was stirred overnight to give a clear blue solution. The volume of the solution at this stage was about 3 mL due to evaporation of the solvent. To this clear blue solution was added 50.0 mg of solid $NH_4(PF_6)$ (0.30 mmol), which resulted in immediate precipitation. The precipitate was redissolved by addition of 2.0 mL of MeCN, and the resulting clear solution was diluted with an additional 10 mL of MeOH. Slow evaporation of this solution at room temperature afforded large blue crystalline cubes of **1** in 5 days. The crystals were harvested by filtration and washed with MeOH (50.0 mg, yield 90%). FTIR data (2% KBr pellet): 3442 (br, s), 2928 (br, m), 1633 (sh), 1611 (s), 1575 (m), 1483 (s), 1447 (s), 1389 (w), 1366 (w), 1305 (m), 1289 (m), 1251 (m), 1211 (m), 1184 (m), 1161 (m), 1128 (w), 1092 (m), 1067 (w), 1054 (m), 1031 (m), 992 (m), 961 (m), 938 (m), 842 (s), 766 (s), 739 (w), 655 (m), 558 (s), 508 (w), 483 (m), 424 (m). Anal. Calcd for $[(CuCl)_3(C_{60}N_{10}H_{60})](PF_6)_3\cdot 5H_2O$: C, 41.34; H, 4.05; N, 8.04. Found: C, 41.36; H, 3.97; N, 8.04 [MW = 1743 g/mol]. High-resolution ESI-MS for monocation $[(CuCl)_3(C_{60}N_{10}H_{60})(PF_6)_2]^+$: Calcd: 1504.1240. Found: 1504.1279 (see the SI).

**Synthesis of $[(CuCl)_3L](PF_6)(ReO_4)_2\cdot 3H_2O$ (2).** A 10.0 mg sample of **1** (0.00573 mmol) was dissolved in 2 mL of MeCN at room temperature. To the resulting clear blue solution was added 5.2 mg of $NaReO_4$ (0.0189 mmol, 3.3 equiv) dissolved in 5 mL of MeOH. Slow evaporation of the resulting clear solution at room temperature afforded large blue crystalline plates of **2** over 3 days. The crystals were harvested by filtration and washed with MeOH (10.0 mg, yield 91%). FTIR data (2% KBr pellet): 3450 (br, s), 2932 (br, m), 1699 (m), 1630 (sh), 1610 (s), 1573 (m), 1482 (s), 1445 (s), 1383 (w), 1367 (m), 1302 (m), 1288 (m), 1248 (m), 1210 (m), 1183 (m), 1159 (m), 1127 (w), 1090 (m), 1067 (w), 1053 (m), 1030 (m), 993 (m), 959 (m), 910 (s), 840 (s), 768 (s), 732 (w), 654 (m), 557 (s), 507 (w), 483 (m), 422 (m). Anal. Calcd for $[(CuCl)_3(C_{60}N_{10}H_{60})](PF_6)(ReO_4)_2\cdot 3H_2O$: C, 37.58; H, 3.47; N, 7.30; Cu, 9.94; Cl, 5.55. Found: C, 37.38; H, 3.47; N, 7.19; Cu, 9.83; Cl, 5.65 [MW = 1917 g/mol].

**X-ray Crystallography.** Data sets for complexes $[(Cu^{II}Cl)_3L](PF_6)_3\cdot 5H_2O$ (**1**), $[(Cu^{II}Cl)_3L](PF_6)(ReO_4)_2\cdot 3H_2O$ (**2**), and $N(CH_2\text{-}o\text{-}C_6H_4CH_2N(CH_2py)_2)_3$ (**L**) were collected as described below. Single crystals suitable for X-ray analysis were coated with Paratone-N oil, suspended in a small fiber loop, and placed in a cold gaseous nitrogen stream on a Bruker APEX CCD X-ray diffractometer performing $\phi$ and $\omega$ scans at 100(2) K. Diffraction intensities were measured using graphite-monochromated Mo Kα radiation ($\lambda$ = 0.71073 Å). Data collection, indexing, initial cell refinements, frame integration, and final cell refinements were accomplished using the program APEX2.[26] Absorption corrections were applied using the program SADABS.[27] Scattering factors and anomalous dispersion corrections were taken from the *International Tables for X-ray Crystallography*. The structure was solved by direct methods using SHELXS[28] and refined against $F^2$ on all data by full-matrix least squares with SHELXL-97[29] following established refinement strategies. Details of the data quality and a summary of the residual values for the refinements are listed in Table S1 in the SI.

Complex **1** crystallizes in the trigonal space group $R\bar{3}$ with $V$ = 14858(3) Å$^3$ and $Z$ = 6. There are two kinds of $PF_6^-$ counteranions in the X-ray structure. P1 is disorder free; P2 sits on a special position and is disordered over two sites. All heavy atoms were refined anisotropically. In the crystal lattice, there are a number of badly disordered solvent molecules. As a result, the PLATON/SQUEEZE function was used to deal with this problem, and the formula of **1** was determined by a combination of X-ray crystallography and elemental analysis. Complex **2** crystallizes in the monoclinic space group $C2$ with $V$ = 7669.0(10) Å$^3$ and $Z$ = 4. The very small Flack parameter 0.029(8) indicates that the correct absolute structure of **2** for this crystal was obtained. The $[(Cu^{II}Cl)_3L]^{3+}$ cation is charge-balanced by one $PF_6^-$ anion and two $ReO_4^-$ anions. A tridentate bridging $ReO_4^-$ anion binds to three Cu atoms, each from a different molecule of **2** through three Cu−O bonds, whereas the other $ReO_4^-$ anion is held in the cavity of a tricopper unit backbone by Coulombic and possible anion−$\pi$ interactions. The $PF_6^-$ anion was not disordered. All heavy atoms in the structure of **2** were refined anisotropically. The largest diffraction peak and hole, 3.621 and −2.129 e Å$^{-3}$, are located close to the Re1 atom (1.03 and 0.77 Å, respectively) and possibly arise from imperfect absorption corrections, as is often encountered in heavy-metal-atom structures. In the X-ray


dx.doi.org/10.1021/ic201172r |*Inorg. Chem.* 2011, 50, 9499–9507

structure of **2**, no solvent molecules were located in the difference electron density maps, but three water molecules were suggested based on elemental analysis (see above). Ligand **L** crystallizes in the trigonal space group $R\bar{3}$ with $V$ = 32725(7) Å$^3$ and $Z$ = 24. There are two molecules in the asymmetric unit, one on a special position with a crystallographically required $C_3$ axis passing through the central N atom and the other at a general position. The PLATON/SQUEEZE function was also used to treat solvent distribution disorder in the X-ray structure of **L**. The identity and purity of **L** were further confirmed by high-resolution ESI-MS.

**Anion Exchange Studies.** Anion exchange of **1** with $NaReO_4$ was achieved by immersing crystals (10.0 mg) in 1.0 mL of a 0.1 M $NaReO_4$ methanolic solution at room temperature without stirring. The exchange process was complete in 1 day as judged by IR spectroscopy, and blue crystals of **1**−$ReO_4$ were harvested by filtration and washed with MeOH (5 × 10 mL) (10.3 mg, yield 91%). FTIR data (2% KBr pellet): 3440 (br, s), 2930 (br, m), 1632 (sh), 1610 (s), 1574 (m), 1482 (s), 1445 (s), 1386 (w), 1368 (w), 1303 (m), 1288 (m), 1251 (m), 1210 (m), 1184 (m), 1159 (m), 1127 (w), 1090 (m), 1067 (w), 1053 (m), 1030 (m), 993 (m), 962 (m), 909 (s), 863 (w), 766 (s), 733 (w), 655 (m), 512 (w), 483 (m), 424 (m). Anal. Calcd for $[(CuCl)_3(C_{60}N_{10}H_{60})](ReO_4)_3$: C, 36.60; H, 3.07; N, 7.11; Cu, 9.68; Cl, 5.40. Found: C, 36.83; H, 3.28; N, 7.07; Cu, 9.33; Cl, 5.90 [MW = 1969 g/mol].

The reversibility of this anion exchange process was studied by exposing crystals of **1**−$ReO_4$ to 1.0 mL of a 0.1 M $NaPF_6$ methanolic solution. The $PF_6^- \leftrightarrow ReO_4^-$ anion exchange processes were repeated three times without the loss of anion exchange activity. Anion exchange between **1** and $NaClO_4$ or $NaIO_4$ was also attempted under the same conditions. All materials after anion exchange were harvested by filtration, washed with methanol, dried in air, and analyzed by IR spectroscopy.

**Powder X-ray Diffraction (PXRD) Studies.** PXRD patterns were recorded with a PANalytical X'Pert Pro Materials research diffractometer equipped with a $\theta/2\theta$ Bragg−Brenano geometry and using nickel-filtered Cu Kα radiation ($K\alpha_1$ = 1.5406 Å, $K\alpha_2$ = 1.5444 Å, and $K\alpha_2/K\alpha_1$ = 0.5). Crystals of **1** were removed from the methanol solution by a pipet and deposited onto a zero-background silicon plate coated with a thin layer of petroleum jelly. The excess solution was removed using a Kimwipe, and the crystals were crushed carefully into the jelly. Crystals of **1**−$ReO_4$ and **1** obtained from anion exchange were loaded and analyzed in a similar manner. Authentic crystalline samples of $NH_4Cl$, $NH_4(PF_6)$, $NaPF_6$, and $NaReO_4$ were also analyzed by PXRD to confirm that no such salts used or generated during synthesis or anion exchange remained on the surface of crystals of **1**, **1**−$ReO_4$, or **1** from anion exchange. PXRD data of these samples are reported in the SI.

## RESULTS AND DISCUSSION

**Synthesis and Structure of Complex 1.** Recently, we reported the assembly of trimetal-phosphate clusters that are structural analogues of the trinuclear metal active sites of many enzymes involved in phosphate metabolism, using a novel multidentate tripodal ligand $N(CH_2\text{-}o\text{-}C_6H_4CH_2N(CH_2py)_2)_3$ (**L**).[25] The three dpa-based arms of **L** can each coordinate a metal ion, and the resulting trinuclear metal site is able to capture a phosphate group, a monoprotonated ($HPO_4^{2-}$) phosphate group, or even a diprotonated ($H_2PO_4^-$) phosphate group, by forming three metal−oxygen bonds. These results clearly demonstrate the capability of the tris-dpa ligand to coordinate a trimetal−tetraoxoanion unit, with the tetraoxoanion acting as a tridentate bridging group. Because of our interest in trapping pertechnetate ion with extremely tight binding as a means for the regulation and removal of this dangerous and radioactive anionic pollutant, we decided to synthesize new trimetallic species, such as tricopper complexes, and then study their potential to capture pertechnetate ion. We chose copper because of its earth abundance and strong binding affinity for hard O atoms.

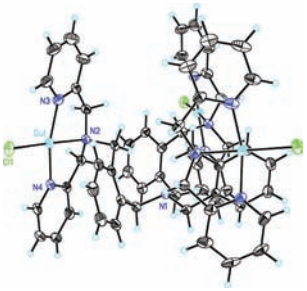

**Figure 1.** Thermal ellipsoid plot (50% probability) of the tricopper $[(CuCl)_3L]^{3+}$ unit of **1**.

**Table 1. Bond Distances (Å) to the Cu Ions in 1 and 2**

| Complex | 1 | 2 | | |
|---|---|---|---|---|
| | Cu1 | Cu1 | Cu2 | Cu3 |
| Cu−N | 1.982(3) | 1.979(8) | 1.996(10) | 1.995(8) |
| Cu−N | 1.997(3) | 1.991(8) | 2.014(11) | 1.996(9) |
| Cu−N | 2.038(3) | 2.049(8) | 2.025(8) | 2.068(8) |
| Cu−Cl | 2.2536(9) | 2.231(3) | 2.214(3) | 2.226(3) |
| Cu−Cl for **1** | 2.7618(9) | | | |
| Cu−O for **2** | | 2.399(6) | 2.270(7) | 2.376(7) |

Slow evaporation of a DCM/hexane (1:5 in volume) solution of free ligand **L** at −10 °C afforded large colorless crystals in 3 weeks. The three ligand arms linked at the ortho positions of the tris(*o*-xylyl) scaffold each carry a dpa unit (Figure S5 in the SI), and these arms fold to give a cavity suitable for trapping anions. Reaction of **L** and 3 equiv of $CuCl_2$ in methanol gave a clear blue solution. Addition of $NH_4(PF_6)$ caused immediate precipitation, and recrystallization of the blue precipitate from MeCN/MeOH afforded large blue cubes of **1** in high yield (90%). The tricopper unit in **1** sits on a special position, with a crystallographically required $C_3$ axis passing through the central N atom (N1, see Figure 1). The three symmetry-equivalent dpa ligand arms each incorporate one Cu ion through three N atoms with characteristic $Cu^{II}$−N single bond lengths (Table 1). Each Cu ion has an additional Cl ligand at a $Cu^{II}$−Cl bond distance of 2.2536(9) Å. The resulting tricopper unit, $[(CuCl)_3L]^{3+}$, is charge-balanced by three $PF_6^-$ anions, which were also located in the X-ray structure.

In the crystal lattice of **1**, two arms of two tricopper ions are connected to one another through a $Cu(\mu\text{-}Cl)_2Cu$ quadrilateral, at a Cu···Cu separation of 3.432 Å (Figure 2B). The bridging of the two $Cl^-$ ions is unsymmetrical. For each dinuclear unit, one chloride ligand is equatorial to its bound $Cu^{2+}$ ion but resides on the axial position of the other $Cu^{2+}$ ion with a longer $Cu^{II}$−Cl distance of 2.7618(9) Å (Table 1). As a result, the $Cu^{2+}$ ion has distorted square-pyramidal coordination geometry. These interactions extend the molecular structure to form an infinite 2-D layer. As shown in Figure 2C, the layer consists of an array of hexagons with a diameter of ∼20 Å. The central N1 atoms of the bridged tricopper units sit at the vertices of these hexagons, with the two arms linked by $\{Cu(\mu\text{-}Cl)_2Cu\}^{2+}$ units forming the


dx.doi.org/10.1021/ic201172r |*Inorg. Chem.* 2011, 50, 9499–9507

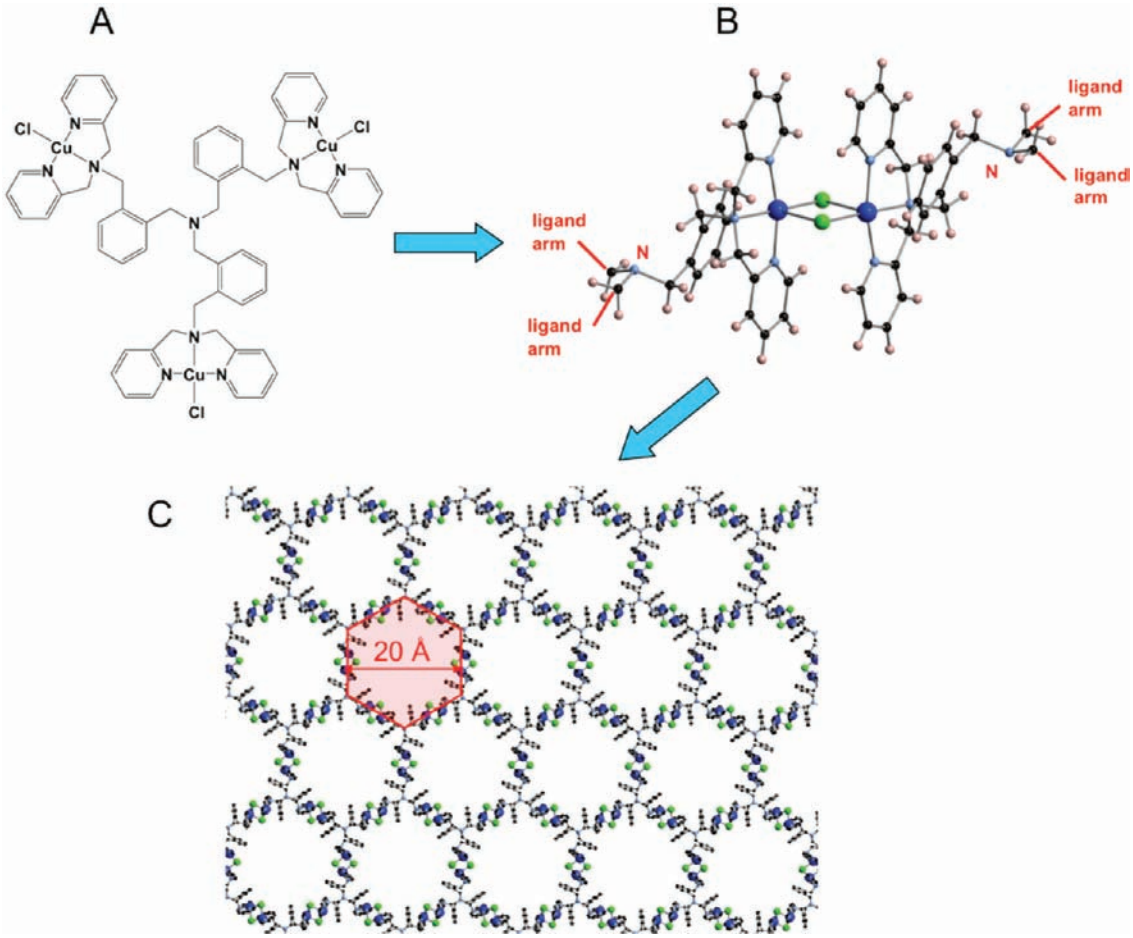


**Figure 2.** (A) Structure of the tricopper $[(Cu^{II}Cl)_3\mathbf{L}]^{3+}$ unit in **1**. (B) Ball-and-stick representation of the $\{Cu(\mu\text{-}Cl)_2Cu\}^{2+}$ unit that bridges two arms of two molecules in **1**. The bridging of the two $Cl^-$ ions is unsymmetrical. (C) 2-D cationic layer extending through $\{Cu(\mu\text{-}Cl)_2Cu\}^{2+}$ interactions. Color code: Cu, blue; Cl, green; N, light blue; C, black; H, pink. The hexagonal pores have diameters of ~20 Å.

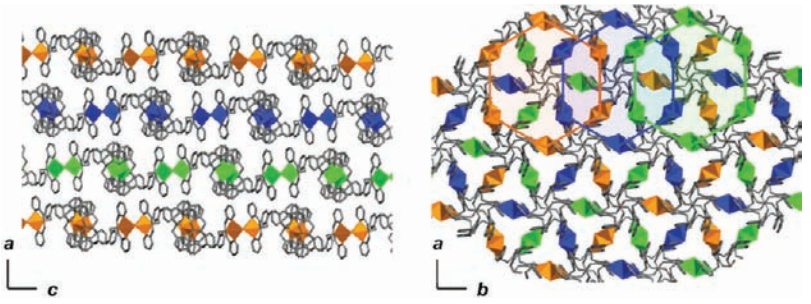


**Figure 3.** Combined polyhedron and stick representations showing the ABCABC... packing of cationic layers in the 3-D structure of **1** viewed along *b* (left) and *c* (right). The coordination spheres of the $Cu^{2+}$ ions are depicted as polyhedra, and the ligand backbone is shown as sticks. H atoms are omitted for clarity. The layers are indicated in orange, blue, and green to distinguish their packing positions.

edges. Because the layers are constructed exclusively with tricopper $[(CuCl)_3\mathbf{L}]^{3+}$ units, the extended structure is positively charged, forming a cationic 2-D MOF.

These cationic layers pack in an ABCABC... manner, with $PF_6^-$ counteranions located within the interlayer spaces. Figure 3 reveals that the tricopper(II) backbones in each 2-D layer have alternating up and down orientations. Because these layers do not overlap with one another, there are no hexagonal channels in the crystal structure. Because there are only weak electrostatic interactions between $PF_6^-$ anions and the cationic MOF, we expected that these guests would be readily exchanged with other anions of interest (vide infra).

**Synthesis and Structural Characterization of Complex 2.** After analyzing the structure of **1**, we were interested to explore its potential to serve as a pertechnetate trapping reagent, anticipating that it might capture a tetrahedral oxoanion in the cavity formed by its tripodal backbone via Cu−O bonds, similar to our previous findings.[25] Because technetium is radioactive with a long half-life (~$10^6$ years), we decided to use perrhenate as a model of pertechnetate for these studies. Table 2 reveals that


dx.doi.org/10.1021/ic201172r |*Inorg. Chem.* 2011, 50, 9499–9507

**Table 2. Structural Properties and Ionic Radii of Tetrahedral $X^{VII}O_4^-$ Anions**

| | ionic radius of $X^{VII}$ (Å) | $X^{VII}$–O bond length (Å) | $X^{VII}O_4^-$ ionic radius (Å) |
|---|---|---|---|
| $TcO_4^-$ | 0.56[a] | 1.711[b] | 2.55[e] |
| $ReO_4^-$ | 0.53[a] | 1.719[b] | 2.60[e] |
| $IO_4^-$ | 0.53[a] | 1.726[c] | 2.50[e] |
| $ClO_4^-$ | 0.27[a] | 1.440[d] | 2.40[e] |

[a] The ionic radius of X in the tetrahedral ion (X = Tc, Re, I and Cl).[30] [b] Tc–O and Re–O bond lengths.[31] [c] The I–O bond length averaged from 21 structures in the Cambridge Crystallographic Data Centre (CCDC). [d] Cl–O distance averaged from more than 50 structures in the CCDC. [e] The effective $X^{VII}O_4^-$ ionic radius.[1,32]

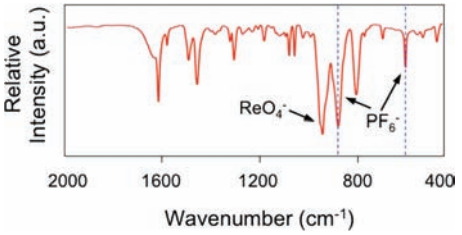


**Figure 4.** FTIR spectrum of complex **2**. Both $ReO_4^-$ and $PF_6^-$ anions are apparent.

the geometric features of perrhenate and pertechnetate, including the radii of the metal center,[30] metal–oxo bond lengths,[31] and effective ionic radii of the two tetraoxoanions,[1,32] are very similar. Because they have the same tetrahedral geometry, similar charge density, and closely related chemical properties, perrhenate is a good model of pertechnetate and should behave in a nearly identical manner in anion trapping studies.

Reaction of **1** with 3 equiv of $NaReO_4$ in MeCN/MeOH and subsequent slow evaporation of the resulting clear blue solution gave a high yield (91%) of large blue plates of **2**. These crystals were harvested by filtration and washed with MeOH before analysis. IR spectra showed the presence of both $ReO_4^-$ (910 $cm^{-1}$) and $PF_6^-$ (840 and 558 $cm^{-1}$) anions in **2** (Figure 4),[33] an indication that perrhenate is trapped in this material. Crystallographic studies revealed that **2** crystallizes in the monoclinic space group *C*2 (Table S1 in the SI) with a tricopper unit almost identical with that of **1**. The three ligand arms of **2** each bind one $Cu^{2+}$ ion through three N atoms, and each Cu ion has an additional chloride ligand. $Cu^{II}$–N and $Cu^{II}$–Cl bond lengths in **2** are comparable to those in **1** (Table 1). Although the three arms of **2** are not symmetry-equivalent in the crystal structure, they are chemically identical. A thermal ellipsoid plot of the tricopper $[(CuCl)_3L]^{3+}$ unit in **2** is depicted in Figure 5.

In **2**, each $[(CuCl)_3L]^{3+}$ unit is charge-balanced by two $ReO_4^-$ and one $PF_6^-$ anions, which were all located in the crystal structure without any disorder. As shown in Figure 6, one $ReO_4^-$ anion is located in the cavity of the tricopper backbone. However, unlike the phosphate derivatives reported previously,[25] for which $H_xPO_4^{(3-x)-}$ ($x$ = 0, 1, or 2) can bridge three metal centers through three metal–oxygen bonds, the long Cu···O(Re) distances (4.580, 4.646, and 4.785 Å) indicate that this $ReO_4^-$ anion (Re2) does not covalently bind to copper but is held electrostatically by the $[(CuCl)_3L]^{3+}$ unit through Coulombic and possible

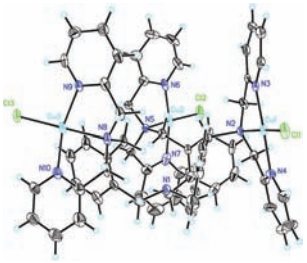

**Figure 5.** Thermal ellipsoid plot (50% probability) of the tricopper $[(CuCl)_3L]^{3+}$ unit in **2**.

anion–$\pi$ interactions. The use of positively charged receptors for the complexation of anions, such as pertechnetate and perrhenate, is an important research area in supramolecular chemistry.[2,17] Because pertechnetate and perrhenate are considered soft bases with low surface charge density, receptors having transition-metal cations are attractive as trapping agents for these two anions. For example, metal complexes of cyclotriveratrylenes (CTVs) having the general formula $[(ML)_3(CTV)]^{6+}$ (M = $Ru^{II}$ or $Fe^{II}$, L = arene) can bind a $ReO_4^-$ anion in their bowl-shaped molecular cavity.[34–36] In our tripodal system, the three Cu-containing arms of **2** fold to form a preorganized cavity that can encapsulate a $ReO_4^-$ anion through electrostatic interactions. A space-filling model (Figure 6C) further reveals the size compatibility between the guest tetrahedral $ReO_4^-$ anion and the tripodal host molecule.

Of further interest is the ability of the other $ReO_4^-$ anion (Re1) to bridge the ligand arms of three molecules of **2**. As shown in Figure 7B, the Re1 perrhenate ion serves as a tridentate bridging unit, with three of its O atoms each connected to a Cu ion from each of three different molecules. The perrhenate O atom resides on the axial position of each Cu center to produce a distorted square-pyramidal geometry, and the resulting Cu–O bond distances are 2.274(7), 2.371(7), and 2.399(6) Å. Because of its low surface charge density, perrhenate is in general not a good $\sigma$-donating ligand to transition-metal ions. Numerous examples of free perrhenate, monodentate, bidentate, or bridging bidentate $ReO_4^-$ anions are known in the literature, but a structurally characterized tridentate bridging $ReO_4^-$ unit is extremely rare.[33,37] The $Cu_3(\mu^3\text{-}ReO_4)$ cluster in **2** is one such example of a tridentate bridging $ReO_4^-$ anion. Apart from these interesting structural features, the tridentate binding of a perrhenate ion in the present structure significantly impacts the immobilization of the anion and as such is a model for pertechnetate trapping. As stated above, the capture of these two anions is difficult, and the need to trap them with tight binding units is an important goal in materials science.[2]

The intermolecular interactions described above extend the structure of **2** to form infinite 2-D layers (Figure 7C). The different solid-state structures of **1** and **2** reveal the consequences of using different linkers to bridge the tricopper $[(CuCl)_3L]^{3+}$ unit in the formation of MOFs. Compared to the relatively short Cu···Cu separation of 3.432 Å in **1**, the three Cu···Cu vectors in the bridged $Cu_3(\mu^3\text{-}ReO_4)$ cluster of **2** have an average value of 6.274 Å. Figure 8 shows the packing of these cationic layers in the crystal lattice. Two layers having opposite orientations form a bilayer structure through weak electrostatic interactions between perrhenate anions in one layer and the ligand backbone in the other. As a result, the two kinds of perrhenate anions, now designated Re1 and Re2, are both trapped in bilayers, with the


dx.doi.org/10.1021/ic201172r |*Inorg. Chem.* 2011, 50, 9499–9507

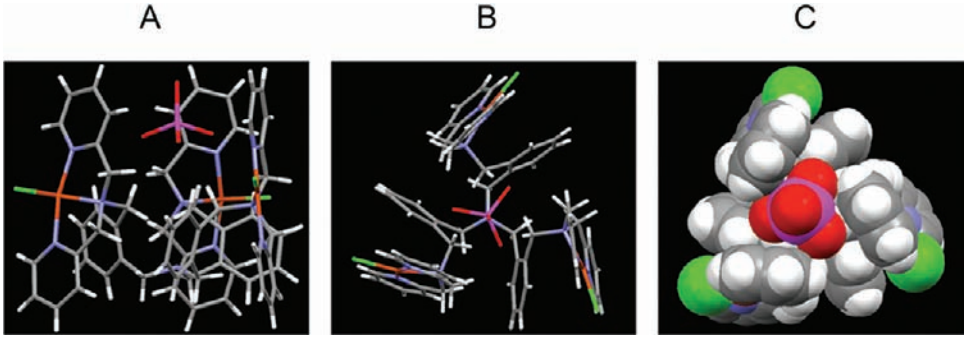


**Figure 6.** (A) Side view of the stick model showing a trapped $ReO_4^-$ anion in the cavity of the tricopper unit backbone of complex **2**. (B) Top view of the trapped $ReO_4^-$ anion in a stick model. (C) Top view of the trapped $ReO_4^-$ anion in a space-filling model. Color code: Re, purple; O, red; Cu orange; Cl, green; N, blue; C, gray; H, white.

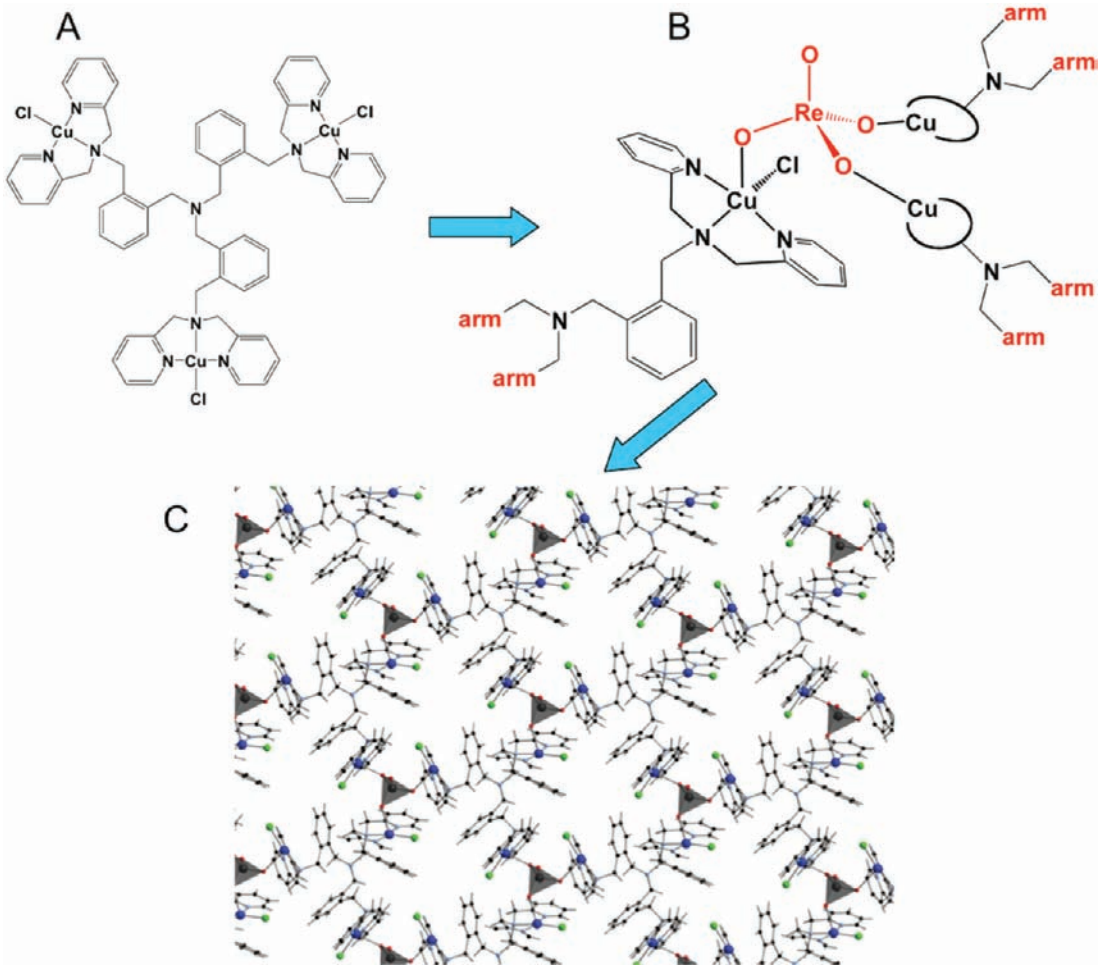


**Figure 7.** (A) ChemDraw structure of the tricopper $[(Cu^{II}Cl)_3\mathbf{L}]^{3+}$ unit of **2**. (B) ChemDraw representation of the $Cu_3(\mu^3\text{-}ReO_4)$ unit that bridges three arms of three molecules of **2**. The perrhenate oxo ligand sits on the axial position of each Cu ion. (C) Combined polyhedron and ball-and-stick representation showing the 2-D layer extended through $Cu_3(\mu^3\text{-}ReO_4)$ interactions. Color code: $ReO_4^-$, gray tetrahedra; O, red; Cu, blue; Cl, green; N, light blue; C, black; H, light pink.

Re1 anions integrated into the 2-D framework via strong covalent bonds and the Re2 anions encapsulated into the tricopper units cavities through Coulombic interactions. The bilayers are positively charged, and they pack in the 3-D structure against anionic layers of $PF_6^-$ anions. The structure of **2**, with alternating bilayers and $PF_6^-$ ions, is presented in Figure 8C.

**Anion Exchange Studies.** Cationic MOFs with positively charged extended networks and loosely bound anionic guests are of potential interest as agents for trapping and removing anionic pollutants.[6,21−24,38,39] Recently, the anion exchange properties of a few such cationic 2-D MOFs have been described.[6,22] Similar to layered double hydroxides with anion exchange and trapping


dx.doi.org/10.1021/ic201172r |*Inorg. Chem.* 2011, 50, 9499–9507

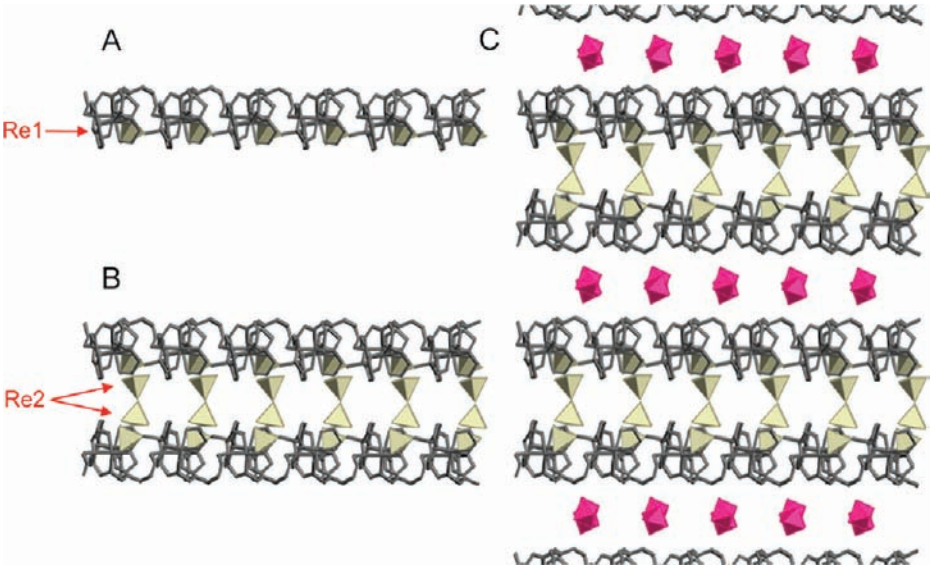


**Figure 8.** Combined polyhedron and stick representations of the monolayer (A), bilayer (B), and 3-D structure (C) of complex **2**. The ligand backbones are shown in sticks; $ReO_4^-$ anions are shown as gray tetrahedra, and $PF_6^-$ anions are shown as purple octahedra. H and C atoms that are not in the main framework skeleton are omitted for clarity.

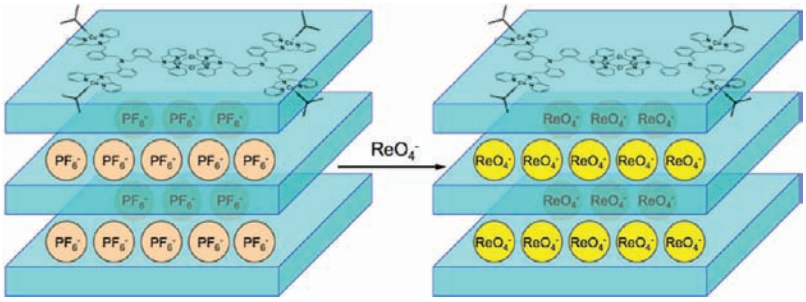


**Figure 9.** Schematic representation showing the interlamellar $PF_6^-$ anions in complex **1** that are exchanged with $ReO_4^-$ anions.

features that have been extensively studied over the last two decades, the interlamellar anion guests in cationic 2-D MOFs are also exchangeable with anions, including perrhenate and perchlorate. In these examples, cationic 2-D layers pack against counteranions and solvent molecules that occupy interlayer spaces. The weak interactions between these anions and the cationic layers facilitate anion exchange reactions for these materials. Because complex **1** also has an extended 2-D MOF structure, formed by $[(CuCl)_3\mathbf{L}]^{3+}$ units through intermolecular Cu($\mu$-Cl)$_2$Cu linkers (Figures 2 and 3), with unbound $PF_6^-$ counteranions located in the interlayer spaces, we were interested to investigate its potential for anion exchange reactions.

The replacement of $PF_6^-$ anions in **1** by perrhenate was achieved by immersing crystals of **1** in a methanolic solution of $NaReO_4$ at room temperature (Figure 9). Complex **1** is not soluble in methanol. As shown in Figure S9 in the SI, the methanol solution is colorless and the crystals maintain their original shape and morphology throughout the anion exchange process. The $PF_6^- \rightarrow ReO_4^-$ anion exchange was complete in 1 day without stirring when as-isolated crystals of **1** with an average dimension of 0.30 mm were employed. This process could be nicely followed by using IR spectroscopy. The anion exchange process is fast, although it could take up to 1 week in a previously reported system.[6] Direct comparison of rate constants for the anion exchange process is difficult because such heterogeneous reactions depend on many experimental factors including crystal size, stir rate, and temperature. Figure 10 shows the FTIR spectra of **1** and its anion-exchanged product **1**−$ReO_4$. Complex **1** has two intense peaks at 842 and 558 cm$^{-1}$ that are characteristic of octahedral $PF_6^-$ anions. Additional strong peaks in the 1400 and 1700 cm$^{-1}$ region and the peak at 766 cm$^{-1}$ are due to the aromatic phenyl and pyridine rings of **L**. After anion exchange, the two strong $PF_6^-$ peaks disappear, and a new intense band at 909 cm$^{-1}$ appears that is characteristic of the tetrahedral $ReO_4^-$ anion.[33] Except for this change, all of the other peaks from the cationic 2-D layers are unaffected. This result confirms complete replacement of $PF_6^-$ by $ReO_4^-$ anions.

The anion exchange was further investigated by PXRD studies. Although we were unable to obtain a single-crystal X-ray structure of **1**−$ReO_4$, the products after anion exchange are crystalline, as shown in Figure 11. Crystals of **1**−$ReO_4$ gave a different PXRD pattern than crystals of **1**, a finding seen in previous anion exchange studies using cationic 2-D MOFs.[6,21] The change in the PXRD has a structural origin, for example, modification of the interlayer distances upon anion exchange. Replacement of $PF_6^-$ by $ReO_4^-$ is also supported by elemental analyses of samples of **1** and **1**−$ReO_4$ (see the Experimental Section).


dx.doi.org/10.1021/ic201172r |*Inorg. Chem.* 2011, 50, 9499–9507

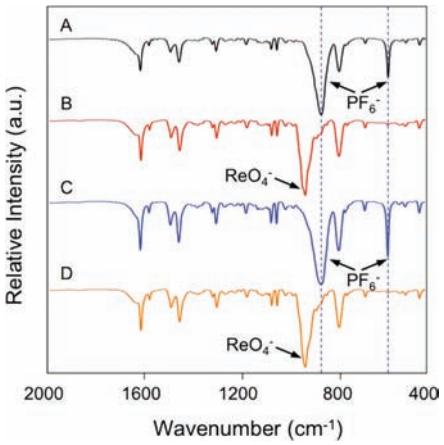


**Figure 10.** FTIR studies of $PF_6^- \leftrightarrow ReO_4^-$ anion exchange: (A) initial complex **1** (black); (B) **1**−$ReO_4$ obtained from anion exchange of A and $NaReO_4$ (red); (C) **1** obtained from anion exchange of B and $NaPF_6$ (blue); (D) **1**−$ReO_4$ obtained from anion exchange of C and $NaReO_4$ (orange). The two peaks from $PF_6^-$ anions are highlighted.

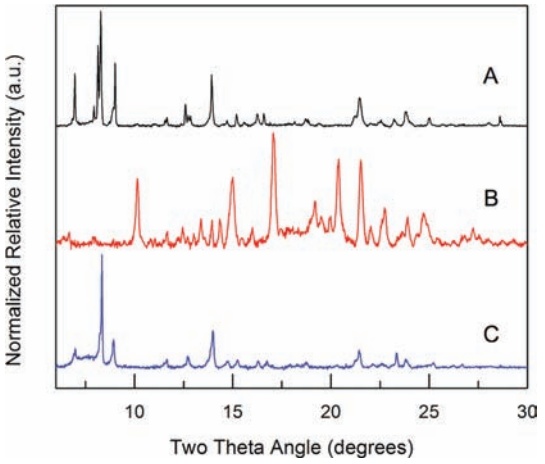


**Figure 11.** PXRD spectra of (A) initial complex **1** (black), (B) **1**−$ReO_4$ obtained from anion exchange of A and $NaReO_4$ (red), and (C) **1** obtained from anion exchange of B and $NaPF_6$ (blue).

The perrhenate in **1**−$ReO_4$ can be back-exchanged with $PF_6^-$ anions. By immersing crystals of **1**−$ReO_4$ in a methanolic solution of $NaPF_6$, we observed that all $ReO_4^-$ anions were replaced by $PF_6^-$ within 1 day at room temperature. As shown in Figure 10 (from B to C), the $ReO_4^-$ peak (909 $cm^{-1}$) in the IR spectrum disappears with appearance of the $PF_6^-$ peaks (842 and 558 $cm^{-1}$). Moreover, crystals of **1** obtained from reaction of **1**−$ReO_4$ with $NaPF_6$ behave similarly to those of **1** synthesized for PXRD (Figure 11) and anion exchange studies (Figure 10D). We repeated the $PF_6^- \rightarrow ReO_4^- \rightarrow PF_6^-$ cycle three times without loss of crystal morphology and anion exchange activity. In these processes, all of the other IR peaks arising from the cationic framework were unchanged.

The anion exchange properties of **1** were also examined using $IO_4^-$ and $ClO_4^-$ anions under the same experimental conditions. The $IO_4^-$ anion has geometric parameters very similar to those of $TcO_4^-$ (Table 2) and is another model for studying pertechnetate trapping. After exchanging $PF_6^-$ anions of **1** with $NaIO_4$ in methanol, blue crystals of **1**−$IO_4$ could be isolated.

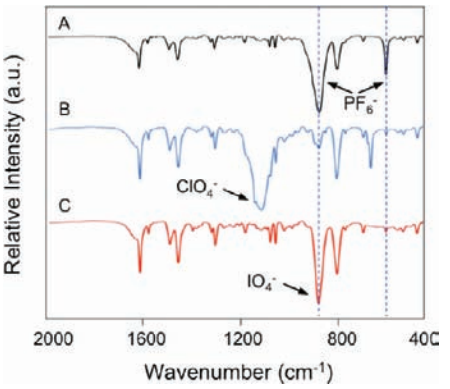


**Figure 12.** FTIR studies of the $PF_6^- \rightarrow XO_4^-$ (X = Cl or I) anion exchange: (A) initial complex **1** (black); (B) **1**-$ClO_4$ obtained from anion exchange of A and $NaClO_4$ (blue); (C) **1**-$IO_4$ obtained from anion exchange of A and $NaIO_4$ (red). The two peaks from $PF_6^-$ anions are highlighted.

These crystals were washed carefully with methanol and then analyzed by IR spectroscopy (Figure 12). A strong peak at 847 $cm^{-1}$ after anion exchange is attributed to $IO_4^-$ anions.[40,41] This assignment is based on literature IR studies of $NaIO_4$. Although the peak is close to one of the peaks of $PF_6^-$ at 842 $cm^{-1}$, complete $PF_6^- \rightarrow IO_4^-$ exchange was confirmed by the disappearance of the peak at 558 $cm^{-1}$ arising from the $PF_6^-$ anions. Similarly, the exchange of $PF_6^-$ for $ClO_4^-$ was investigated. Complex **1**−$ClO_4$ displays a new peak at 1090 $cm^{-1}$ that is characteristic of $ClO_4^-$ anions.[42,43] In both anion exchange processes, all other peaks were unaffected. These results further demonstrate the ability of **1** to exchange its interlamellar anions.

## SUMMARY AND CONCLUSIONS

We report here the crystal structure of a multidentate tripodal ligand $N(CH_2\text{-}o\text{-}C_6H_4CH_2N(CH_2py)_2)_3$ (**L**) and two MOFs with trapped anions, $[(CuCl)_3\mathbf{L}](PF_6)_3\cdot 5H_2O$ (**1**) and $[(CuCl)_3\mathbf{L}](PF_6)(ReO_4)_2\cdot 3H_2O$ (**2**). Compound **1** has a 2-D layer structure formed by tricopper $[(Cu^{II}Cl)_3\mathbf{L}]^{3+}$ units extended through intermolecular $Cu(\mu\text{-}Cl)_2Cu$ linkers. The $PF_6^-$ counteranions are located within interlayer spaces and can be exchanged with other anions, including perrhenate, perchlorate, and periodate. These results suggest that **1** is an efficient anion-exchanging reagent. Compound **2** also has a layered 2-D structure, but its tricopper $[(Cu^{II}Cl)_3\mathbf{L}]^{3+}$ units are extended through intermolecular $Cu_3(\mu^3\text{-}ReO_4)$ linkages. The tridentate bridging perrhenate unit represented in the $Cu_3(\mu^3\text{-}ReO_4)$ cluster is extremely rare, probably because of the low surface charge density of the perrhenate ion and its corresponding poor $\sigma$-donor properties. The second perrhenate anion in **2** is located in a cavity formed by the tricopper unit backbone and held in place by Coulombic interactions. As a consequence, in addition to perrhenate trapping through electrostatic interactions, **2** represents an exceptional example of tight binding of perrhenate ion through the formation of three covalent Cu−O bonds and the integration of $ReO_4^-$ anions into the network skeleton. The immobilization of perrhenate in extended structures, such as MOFs, provides a promising lead for pertechnetate trapping studies, and the present investigation may therefore offer some strategic guidance for the regulation of anionic pollutants.


dx.doi.org/10.1021/ic201172r |*Inorg. Chem.* 2011, 50, 9499–9507

## ■ ASSOCIATED CONTENT

**Supporting Information.** $^{1}H$ and $^{13}C$ NMR, high-resolution ESI-MS, FTIR, and diffuse-reflectance spectra, thermal ellipsoid plot, crystal data and structure refinement parameters, PXRD patterns, and photographs of anion exchange. This material is available free of charge via the Internet at http://pubs.acs.org.

## ■ AUTHOR INFORMATION

**Corresponding Author**
*E-mail: lippard@mit.edu.

## ■ ACKNOWLEDGMENT

We thank the Camille and Henry Dreyfus Foundation for financial support, Professor Daniel G. Nocera for the use of his Praying Mantis accessory, and Professor Mircea Dincă for many helpful suggestions. We also thank Dr. Natalia Shustova for helpful discussions about PXRD.

## ■ REFERENCES

(1) Gloe, K.; Stephan, H.; Grotjahn, M. *Chem. Eng. Technol.* **2003**, *26*, 1107–1117.
(2) Katayev, E. A.; Kolesnikov, G. V.; Sessler, J. L. *Chem. Soc. Rev.* **2009**, *38*, 1572–1586.
(3) Kim, S. K.; Sessler, J. L. *Chem. Soc. Rev.* **2010**, *39*, 3784–3809.
(4) Gale, P. A. *Chem. Soc. Rev.* **2010**, *39*, 3746–3771.
(5) Ballester, P. *Chem. Soc. Rev.* **2010**, *39*, 3810–3830.
(6) Fei, H. H.; Rogow, D. L.; Oliver, S. R. J. *J. Am. Chem. Soc.* **2010**, *132*, 7202–7209.
(7) Wang, S. A.; Alekseev, E. V.; Juan, D. W.; Casey, W. H.; Phillips, B. L.; Depmeier, W.; Albrecht-Schmitt, T. E. *Angew. Chem., Int. Ed.* **2010**, *49*, 1057–1060.
(8) Yu, P.; Wang, S.; Alekseev, E. V.; Depmeier, W.; Hobbs, D. T.; Albrecht-Schmitt, T. E.; Phillips, B. L.; Casey, W. H. *Angew. Chem., Int. Ed.* **2010**, *49*, 5975–5977.
(9) Wolff, J. *Pharmacol. Rev.* **1998**, *50*, 89–105.
(10) Urbansky, E. T. *Environ. Sci. Pollut. Res.* **2002**, *9*, 187–192.
(11) Greer, M. A.; Goodman, G.; Pleus, R. C.; Greer, S. E. *Environ. Health Perspect.* **2002**, *110*, 927–937.
(12) Zayed, A. M.; Terry, N. *Plant Soil* **2003**, *249*, 139–156.
(13) Costa, M.; Klein, C. B. *Crit. Rev. Toxicol.* **2006**, *36*, 155–163.
(14) Oliver, S. R. J. *Chem. Soc. Rev.* **2009**, *38*, 1868–1881.
(15) Mark, R.; Findley, W. N. *Polym. Eng. Sci.* **1978**, *18*, 6–15.
(16) Sessler, J. L.; Kim, S. K.; Gross, D. E.; Lee, C. H.; Kim, J. S.; Lynch, V. M. *J. Am. Chem. Soc.* **2008**, *130*, 13162–13166.
(17) Thuéry, P. *Inorg. Chem.* **2009**, *48*, 4497–4513.
(18) Chibwe, K.; Jones, W. *J. Chem. Soc., Chem. Commun.* **1989**, 926–927.
(19) Rives, V.; Ulibarri, M. A. *Coord. Chem. Rev.* **1999**, *181*, 61–120.
(20) Poudret, L.; Prior, T. J.; McIntyre, L. J.; Fogg, A. M. *Chem. Mater.* **2008**, *20*, 7447–7453.
(21) Min, K. S.; Suh, M. P. *J. Am. Chem. Soc.* **2000**, *122*, 6834–6840.
(22) Hamilton, B. H.; Wagler, T. A.; Espe, M. P.; Ziegler, C. J. *Inorg. Chem.* **2005**, *44*, 4891–4893.
(23) Xu, G. C.; Ding, Y. J.; Okamura, T. A.; Huang, Y. Q.; Liu, G. X.; Sun, W. Y.; Ueyama, N. *CrystEngComm* **2008**, *10*, 1052–1062.
(24) Michaelides, A.; Skoulika, S. *Cryst. Growth Des.* **2009**, *9*, 2039–2042.
(25) Cao, R.; Müller, P.; Lippard, S. J. *J. Am. Chem. Soc.* **2010**, *132*, 17366–17369.
(26) Bruker AXS. *APEX2 v2009*; Madison, WI, 2009.
(27) Sheldrick, G. M. *SADABS, 2008/1*; University of Göttingen: Göttingen, Germany, 2008.
(28) Sheldrick, G. M. *Acta Crystallogr.* **1990**, *A46*, 467–473.
(29) Sheldrick, G. M. *Acta Crystallogr.* **2008**, *A64*, 112–122.
(30) Shannon, R. D. *Acta Crystallogr.* **1976**, *A32*, 751–767.
(31) Krebs, B.; Hasse, K. D. *Acta Crystallogr.* **1976**, *B32*, 1334–1337.
(32) Marcus, Y. *J. Solution Chem.* **1994**, *23*, 831–848.
(33) Chakravorti, M. C. *Coord. Chem. Rev.* **1990**, *106*, 205–225.
(34) Steed, J. W.; Junk, P. C.; Atwood, J. L.; Barnes, M. J.; Raston, C. L.; Burkhalter, R. S. *J. Am. Chem. Soc.* **1994**, *116*, 10346–10347.
(35) Holman, K. T.; Halihan, M. M.; Jurisson, S. S.; Atwood, J. L.; Burkhalter, R. S.; Mitchell, A. R.; Steed, J. W. *J. Am. Chem. Soc.* **1996**, *118*, 9567–9576.
(36) Gawenis, J. A.; Holman, K. T.; Atwood, J. L.; Jurisson, S. S. *Inorg. Chem.* **2002**, *41*, 6028–6031.
(37) Inglis, R.; Jones, L. F.; Karotsis, G.; Collins, A.; Parsons, S.; Perlepes, S. P.; Wernsdorfer, W.; Brechin, E. K. *Chem. Commun.* **2008**, 5924–5926.
(38) Zhao, W.; Fan, J.; Okamura, T. A.; Sun, W. Y.; Ueyama, N. *Microporous Mesoporous Mater.* **2005**, *78*, 265–279.
(39) Du, M.; Zhao, X. J.; Guo, J. H.; Batten, S. R. *Chem. Commun.* **2005**, 4836–4838.
(40) Gymkowski, T.; Lambert, D. G.; Kimmel, H. S. *J. Inorg. Nucl. Chem.* **1972**, *34*, 1841–1846.
(41) Levason, W. *Coord. Chem. Rev.* **1997**, *161*, 33–79.
(42) Bünzli, J. C. G.; Mabillard, C. *Inorg. Chem.* **1986**, *25*, 2750–2754.
(43) Krasnopoler, A.; Stuve, E. M. *J. Vac. Sci. Technol., A* **1995**, *13*, 1681–1686.